© 2022. Published by The Company of Biologists Ltd | Journal of Experimental Biology (2022) 225, jeb244223. doi:10.1242/jeb.244223

RESEARCH ARTICLE

Visual signals in the wing display of a tephritid fly deter jumping spider attacks

Dinesh Rao[1,*], Skye M. Long[2], Horacio Tapia-McClung[3], Kevin Salgado-Espinosa[1], Ajay Narendra[4], Samuel Aguilar-Arguello[5], Luis Robledo-Ospina[1], Dulce Rodriguez-Morales[1,6] and Elizabeth M. Jakob[2]

ABSTRACT

Visual animal communication, whether to the same or to other species, is largely conducted through dynamic and colourful signals. For a signal to be effective, the signaller must capture and retain the attention of the receiver. Signal efficacy is also dependent on the sensory limitations of the receiver. However, most signalling studies consider movement and colour separately, resulting in a partial understanding of the signal in question. We explored the structure and function of predator–prey signalling in the jumping spider–tephritid fly system, where the prey performs a wing waving display that deters an attack from the predator. Using a custom-built spider retinal tracker combined with visual modelling, as well as behavioural assays, we studied the effect of fly wing movement and colour on the jumping spider's visual system. We show that jumping spiders track their prey less effectively during wing display and this can be attributed to a series of fluctuations in chromatic and achromatic contrasts arising from the wing movements. These results suggest that displaying flies deter spider attacks by manipulating the movement biases of the spider's visual system. Our results emphasise the importance of receiver attention on the evolution of interspecific communication.

KEY WORDS: Predator–prey interactions, Wing interference colouration, Salticid vision, Retina, Spider, Fly

INTRODUCTION

For visual communication to be effective, a signal must attract and hold the attention of the targeted receiver, as well as be interpreted accurately. A number of constraints modulate the efficacy of the signal, such as the receiver's visual capabilities and sensory biases, the medium of transmission and the distance between individuals (Rosenthal, 2007). The incredible variety of movements and colours in peacock spiders (Otto and Hill, 2017) or in the birds of paradise (Ligon et al., 2018) is a testament to the effect of selection in the generation of such displays. The key to triggering the receiver's attention is a combination of display and colour (Rosenthal, 2007), but this has rarely been studied together.

[1]Instituto de Biotecnologia y Ecologia Aplicada, Universidad Veracruzana, 91090 Xalapa, Veracruz, Mexico. [2]Department of Biology, University of Massachusetts, Amherst, MA 01003, USA. [3]Instituto de Investigacion en Inteligencia Artificial, Universidad Veracruzana, 91097 Xalapa, Veracruz, Mexico. [4]School of Natural Sciences, Macquarie University, Sydney, NSW 2109, Australia. [5]New Zealand Forest Research Institute (Scion), Christchurch 8011, New Zealand. [6]Instituo de Neuroetologia, Universidad Veracruzana, 91190 Xalapa, Veracruz, Mexico.

*Author for correspondence (vrao@uv.mx)

D.R., 0000-0002-1900-7742; K.S., 0000-0002-5383-1639; A.N., 0000-0002-1286-5373; S.A., 0000-0003-3138-2948; L.R., 0000-0002-7855-3444; D.R., 0000-0002-0269-8540; E.M.J., 0000-0002-7796-8736

Received 2 March 2022; Accepted 28 November 2022

Visual signals have led to the evolution of different behaviours in various animals in the context of sexual selection and prey attraction, among others. In some cases, prey species find it useful to attract and hold the attention of their potential predators either to advertise their toxicity (aposematism) or to distract predators (Robledo-Ospina and Rao, 2022; Ruxton et al., 2018). This is counterintuitive because prey signalling to the predators is inherently risky. However, prey signalling to predators may reduce the likelihood of a successful attack, either before the attack is launched or during the attack (Ruxton et al., 2018). Prey may also transmit information regarding their body condition (Caro, 1995) or seek to deceive the predator by adopting exaggerated postures that modify their appearance (Brodie, 1977). Signals that are used to deter attacks have been broadly characterised as pursuit deterrence signals (Hasson, 1991). Despite a longstanding interest in the function of these signals, there have been few empirical tests, and fewer still using ecologically relevant predators (Ruxton et al., 2018).

For pursuit deterrent signals to be effective, the movement, form or colouration of the body part must be conspicuous to the predator's visual system. Conspicuousness may be enhanced if the prey has structural colours produced by interference reflection, where visibility is influenced by the angle of light and movement (Kelley et al., 2019; Parker, 1998; Stuart-Fox et al., 2020), but structural colours may also be used as a form of camouflage (Kjernsmo et al., 2020). Wing interference colours (WIC) and wing specularity (i.e. gloss or shine) generated by the transparent part of insect wings may have an anti-predatory function, similar to that seen in the metallic colours of greenbottle flies (Pike, 2015), or constitute a signal for conspecific communication (Eichorn et al., 2017; Hawkes et al., 2019; Schultz and Fincke, 2009; Shevtsova et al., 2011).

We explored the structure and function of predator–prey signalling in the jumping spider–tephritid fly system, where the fly performs a wing waving display that deters an attack from the spider. Tephritid fly wings are generally banded, with pigmented sections interspersed with hyaline segments. The fly's defence against conspecifics and heterospecifics is mainly with wing waving displays termed as supination, where it makes semi-circular loops while waving its wings in a synchronous or asynchronous manner as it approaches the target (see Fig. 1A). The supination display is triggered by the movement of the fly's opponent (either another fly or a predator) and is similar irrespective of the identity of the opponent (Aguilar-Argüello et al., 2015). It has been shown in several studies (Greene et al., 1987; Hasson, 1995; Mather and Roitberg, 1987) that wing displays from tephritid flies deter attacks (up to 90% of spider attacks in the fly *Anastrepha ludens*), but attention has usually been focused on the pigmented fraction of the fly wings (Rao and Díaz-Fleischer, 2012), and there is no information about the effect of fly motion with respect to jumping spider vision.

Journal of Experimental Biology (2022) 225, jeb244223. doi:10.1242/jeb.244223

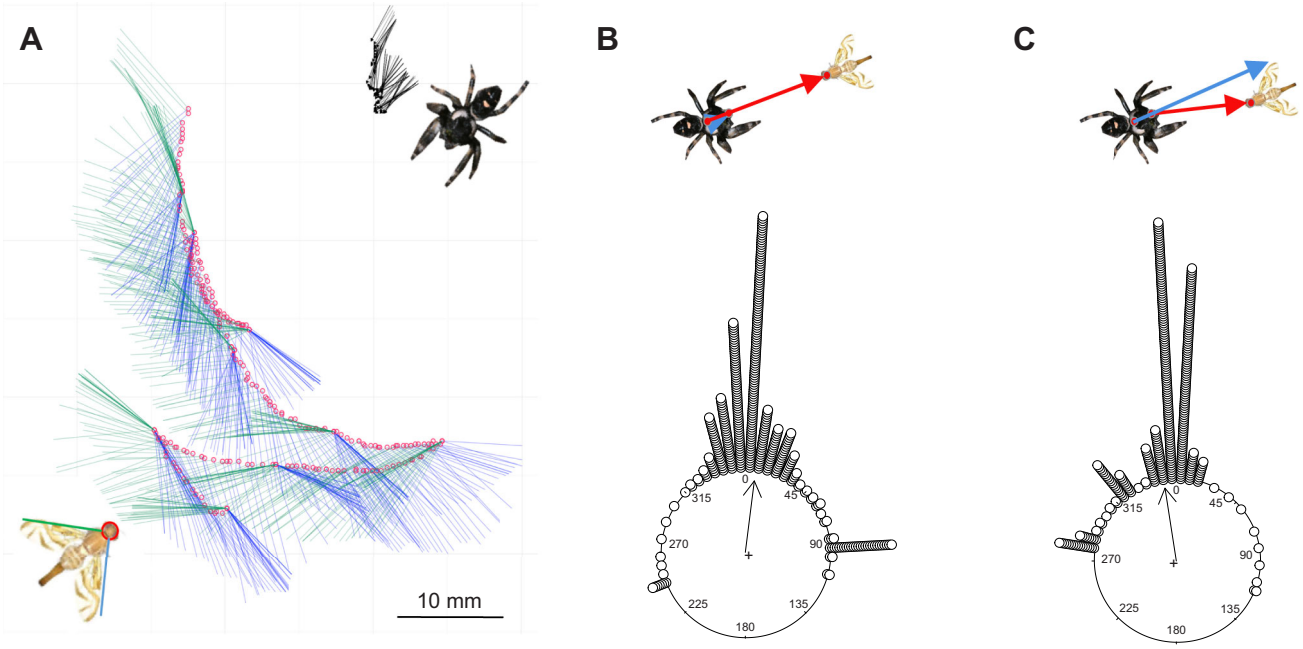

Fig. 1. Head orientation of the spider (*Phidippus audax*) towards displaying and non-displaying Mexican fruit fly (*Anastrepha ludens*). (A) Supination display trajectory of the fly against a jumping spider predator. The red circles represent the head of the fly; the blue and green lines represent the wings. When wings are sustained in the same position, they appear as darker lines. The arrows next to the spider show the body axis (head–tip of the abdomen) of the spider relative to the displaying fly. Note that the fly approaches the spider in semi-looping movements during the display. (B,C) Gaze direction analysis of the principal eyes of the jumping spider when facing (B) a non-displaying (n=10) and (C) a displaying fly (n=9). An error angle of 0 deg implies that the spider gazes were aligned with the head of the fly (i.e. blue and red lines align, see inset in B). Deviation from 0 deg (error angle) implies that spider gazes were focused away from the fly head (i.e. blue and red lines diverge in inset in C).

Jumping spider vision has been reviewed in detail (Harland et al., 2012; Hill, 2022; Morehouse, 2020). Jumping spiders have an unusual distributed visual system with four pairs of eyes, two pairs of which are forward facing (Fig. 2A). Of these forward-facing eyes, the anterior lateral eyes have larger retinae that do not move and serve as excellent motion detectors. The principal eyes have small, boomerang-shaped retinae situated at the proximal end of moveable eye tubes inside the spider's cephalothorax. The eye tubes can move to direct the gaze of the boomerang-shaped retinae to different areas of the visual field. The anterior lateral and principal eyes work in close collaboration, as the anterior lateral eyes are necessary to direct the gaze of the principal eyes (Jakob et al., 2018). When detecting a stimulus of interest, a spider pivots its body to bring the stimulus into the field of view of the forward-facing eyes. The principal eyes can then move to track a moving stimulus or investigate a stimulus while the body remains motionless (Land, 1969), a potentially useful trait for a visually hunting predator.

We hypothesised that the pursuit deterrent effect of a displaying fly can be attributed to changes in the spider's visual attention. To address this, we: (1) analysed the change in body orientation of untethered spiders in an arena as they encountered displaying and non-displaying flies; (2) used a custom-built eyetracker to analyse the gaze direction of a tethered spider's principal eyes as they observed videos of displaying, moving and non-moving flies; and (3) used multispectral digital photography, visual modelling of the acuity and colour perception of the spider, and empirical behavioural assays to evaluate the efficacy of chromatic and achromatic cues in deterring attacks under different light conditions.

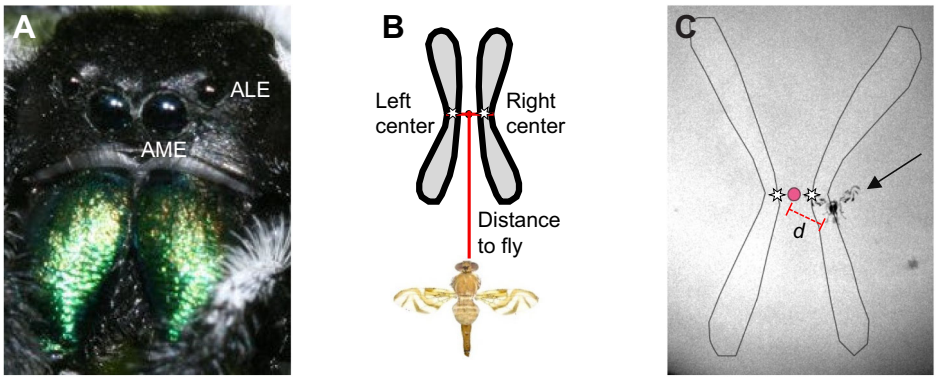

Fig. 2. The principal eyes and retinae of the jumping spider *Phidippus audax*. (A) Frontal view of jumping spider eyes. ALE, anterior lateral eyes; AME, anterior median eyes. (B) Schematic representation of the retinae of the principal eyes (i.e. AME) of the spider and (C) a frame grab showing the retinae and stimulus (i.e. a video of a fly; black arrow). We used the midpoint (red dot) between the centre of the left and right retinae as a proxy for overall retinal movement. The distance (d) between the midpoint and the head of the fly was used in further analysis. Note that the video of the fly was superimposed onto the video recording of retinal response to the stimulus for analysis. See Materials and Methods for details.

Journal of Experimental Biology (2022) 225, jeb244223. doi:10.1242/jeb.244223

MATERIALS AND METHODS

Study species

We used adult female *Phidippus audax* (Hentz 1845) (Araneae: Salticidae) spiders and the Mexican fruit fly (*Anastrepha ludens* Loew 1873; Diptera: Tephritidae). Both species are known to co-occur in citrus orchards in Mexico (Gonzalez-Lopez et al., 2015). The fruit flies frequently congregate on the leaves of citrus plants and are known to employ a lekking mating system where males defend non-resource territories (Aluja et al., 2006). Female flies defend oviposition sites.

Spider orientation to displaying flies in an arena

Spiders were collected from abandoned farms around Xalapa, Mexico, and kept under environmentally enriched conditions (Carducci and Jakob, 2000) in the arthropod laboratory at INBIOTECA, Universidad Veracruzana. Flies were obtained as pupae from the MoscaFrut facility in Metapa de Dominguez, Chiapas, Mexico, and were reared in cages. They were fed with a yeast hydrolosate/sugar mixture and given water *ad libitum* upon emergence. Predator–prey experiments were carried out in the laboratory under natural light conditions (i.e. next to a window with sunlight) by placing a spider and a fly in a glass Petri dish (10 cm diameter) arena, with an opaque partition separating the two. They acclimated for 1 min and the partition was removed for the experiment to begin. The interaction was filmed from above at 25 frames s^{-1} at a resolution of 1920×1080 pixels with a SONY HDR-PJ790V video camera.

From the videos, using a custom MATLAB program (courtesy of Jan Hemmi and Robert Parker; MathWorks, Natick, MA, USA), we manually tracked two points on the spider's cephalothorax and one point on the fly's head. We digitised the anterior (between the spider's principal eyes) and posterior position of the spider cephalothorax and generated *x*,*y* coordinates to determine the approximate gaze direction of the spider's forward-facing principal eyes. Gaze direction is a useful measure of selective attention in invertebrates (Winsor et al., 2021). We note here that cephalothorax movement is a rough proxy of retinal movements, as jumping spider retinae have been shown to have an angular travel of up to 50 deg (Land, 1969; Morehouse, 2020) and it was not possible to control for movement of the eye tubes of the spiders. Nevertheless, a field of view of ±10 deg from the midpoint of the sightline, i.e. a line joining the centre of the principal eyes and the back of the cephalothorax has been used in other studies (Rößler et al., 2021).

We manually separated videos into two categories: (1) where the fly performed a display (n=9; Movie 1) and (2) where there was no display (n=10). For an illustration of a typical display, see Fig. 1A. We analysed these behaviours only when the fly and spider were subjectively observed to be oriented towards each other. To determine the gaze direction of spiders relative to the fly (Fig. 1B,C inset), we calculated the angle formed by the body axis of the spider (i.e. the line connecting the anterior and posterior position of the cephalothorax of the spider) and the line formed between the anterior position of the cephalothorax of the spider and the head of the fly (also known as the line of sight). This angle has also been referred to as the 'error angle' (Collett and Land, 1975). When the spider's gaze was directed to the head of the fly, the angle recorded would be 0 deg. We determined these spider error angles for displaying and non-displaying flies. Because the bout duration varied between individuals (different flies displayed for different periods), we used the first 38 frames of all spiders to determine the error angles. Thirty-eight frames were used because it was the smallest number of frames in common between the videos. The first frame was determined when both spider and fly oriented towards each other. From this, we determined the mean heading direction (ø), length of the mean vector (r) and circular standard deviation in Oriana v 4.0 (Kovach Computing Services, UK). We compared the distribution of the error angle of the spider with respect to displaying and non-displaying flies using a Watson U^2 test (Landler et al., 2021).

Retinal tracking precision of displaying flies

For this experiment, *P. audax* spiders were collected as penultimates or adults from farming fields in western Massachusetts, USA, and housed in enriched environment cages at the University of Massachusetts Amherst. Spiders were fed crickets (*Acheta domesticus*) and had access to water *ad libitum*. Adult female spiders were randomly chosen from the lab population.

To observe the movement of the retinae of the two principal eyes (see Fig. 2A), we used a custom-built spider retina tracking apparatus (hereafter 'eyetracker') at the University of Massachusetts Amherst. The eyetracker and other experimental design details are described in detail elsewhere (Canavesi et al., 2011; Jakob et al., 2018). We provide a brief summary of the setup here.

The eyetracker consists of two main optical elements (Canavesi et al., 2011). Spiders were positioned so that they could look through the eyetracker and view stimuli presented in visible light. The video stimuli were projected onto a Roscoclux frosted diffusion filter (Gel/116, transmission 9%) by an Aaxa P4x Pico Projector. These stimuli did not contain UV information, but previous work confirmed that *P. audax* respond to video lacking UV (Bednarski et al., 2012; Bruce et al., 2021; Jakob et al., 2018). The retinae were illuminated by an IR light, invisible to the spiders, shone into the spider's principal eyes (Thorlabs IR 850 nm Mounted High-Power LED). An EO-1312 mol l^{-1} CMOS monochrome USB camera captured the reflections in IR of the retinae and recorded their motion.

To position spiders in the eyetracker, we tethered them to a plastic micro-brush by a warmed wax mixture (beeswax:resin :: 1:1 mixture) applied to their cephalothorax. The end of the microbrush was clipped to a manual five-way positioner (Thor Labs). To ensure that spiders were positioned so they could see every area of the stimulus screen, we ran a calibration protocol (written in Processing v2.2) in which we checked that spider retinae tracked an image of a square moved to each corner of the screen.

Spiders watched three types of stimulus videos: a still fly (n=14), a moving fly (i.e. non-displaying fly that was walking; n=15) and a displaying fly (n=14). We used three different exemplars of the same behaviour of each stimulus treatment. The flies were filmed from the front (i.e. with the fly facing the camera; see Movie 1) for the still and displaying treatments and from the side for the movement treatment. All flies were filmed with a uniform background. Each spider was presented all three fly video types in a randomised order and individual spiders were tested only once on the treatments. Spiders were exposed to a white screen for 1 min followed by 3 min of a stimulus video, with approximately 5 min of blank screen between treatments in order to allow the spider to rest.

To ensure that the stimulus video and retinal positions were aligned in time, we displayed both simultaneously on the same computer monitor and recorded them together in real time using the screen capture software Debut (v3.07). In post-processing, we then overlaid the stimulus video and retinal video using Final Cut Pro (Apple Inc., Cupertino, CA, USA), using the calibration video to ensure that the alignment was correct. These composite videos were exported to Compressor (v.4) and then saved as image sequences

(.jpg files) at 10 frames s^{-1} (see Movie 2 for a sample video). Using the image sequences, we tracked the *x*,*y* position of the centres of the left and right retinae and the head of the fly (the stimulus) using the MTrackJ plugin for ImageJ (Meijering et al., 2012) (Fig. 2B,C). We chose the head of the fly as the target as a previous study showed that jumping spiders target the head of the prey (Bartos and Minias, 2016). Only the *x* coordinates (i.e. horizontal displacement) were used for subsequent analysis because there is little or no vertical displacement of the fly in the videos as well as under natural conditions (see Fig. S1 for analysis of vertical displacement).

The movements of the two principal-eye retinae of *P. audax* are highly synchronized and spiders direct the high-acuity 'elbow' of the boomerang-shaped retinae toward areas of interest (Jakob et al., 2018), so we used the midpoint of the distance between the retinal centres as a proxy for retinal movement. The midpoint was calculated as the centre of the Euclidian distance between the centres of the two retinae.

Analysis of retinal positions

We used time-series analysis to analyse the data by determining the distance (i.e. separation in pixels) between stimulus and retina coordinates at each time period (i.e. video frame, 10 frames s^{-1}). A distance value of 0 implies that the spider retinae were perfectly tracking the fly's head. Distance data were pooled according to treatments. Because the order of stimulus videos was randomised, there is very little probability that any two spiders would view the fly in the same position at exactly the same time. Missing data (owing to noise in video of retinae) in time and retinal position were dealt with by a third-order Hermite interpolation. We then compared the frequency distributions of distances of all spiders between the three treatments (i.e. display versus moving, display versus still and moving versus still) with a Kolmogorov–Smirnov test (this tests the hypothesis whether the two distributions are drawn from the same population) using Mathematica (Wolfram Research, Inc., Champaign, IL, USA). One outlier in the still treatment was removed owing to a lack of sufficient trackable data.

Optical flow

To quantify and visualise the motion of components of the fly display and movement (including wings and body movements), we used an optical flow algorithm using the ImageDisplacements function in Mathematica to generate a dense motion field. This process compares horizontal and vertical displacement of individual pixels across consecutive frames of a short representative video and computes the magnitude and direction of pixel displacement (Raudies, 2013). Subsequently, these were represented as vectors known as the optical flow vector field. We then used the mean vector over the whole image sequence to present the results in a composite image for a displaying fly and a moving fly.

Wing interference colouration

Image acquisition and analysis

In this experiment, we simulated the appearance of the fly wing in different angles from the perspective of a jumping spider using psychophysical visual modelling techniques. We took photos of detached fly wings at different opening angles relative to the longitudinal body axis of the fly to measure colour variation during the display behaviour. We staged the opening angles with a wing attached to an entomological pin such that the plane of the wing was perpendicular to the ground in order to simulate different wing angles during a display. All other components of the wing position (i.e. yaw, pitch) were kept constant. We photographed the following wing opening angles against a standard grey background: 90, 100, 110, 120, 130, 140 and 150 deg. We measured the relative area of the pigmented part of the wing, the wing specularity and the WIC at different opening angles in ImageJ.

We took two photos at each angle in the UV and visible spectra (~300 to 400 nm and ~400 to 700 nm, respectively) of both wing and head of *A. ludens* from a front view with an Olympus Pen E-PM2 camera (converted to full spectrum, Lifepixel.com) with a UV-transmitting EL-Nikkor 80 mm f/5.6 lens attached. All the photos were taken in laboratory conditions with an Iwasaki EYE Color arc lamp (70 W 1.0 A; Venture Lighting Europe Ltd, Hertfordshire, UK) as light source. The lamp was modified by manually removing the integrated UV filter, which allows the emission of light in the UV spectrum. We did not use a diffusion filter for the lamp.

The ultraviolet photo was created by using a Baader UV pass and infrared (IR)/visible blocking filter, transmitting from ~300 to 400 nm, and the visible spectrum photo, using a UV/IR blocking filter, transmitting between ~400 and 700 nm. Those sets were combined for each angle using the Multispectral Image Calibration and Analysis (MICA) plugin (Troscianko and Stevens, 2015) to create a multispectral image that is a stack of images corresponding to different parts of the spectrum: UV, short wavelength (SW), medium wavelength (MW) and long wavelength (LW).

The multispectral images, with reflectance values in each channel, were transformed to the predicted photoreceptor responses (quantum catch values) for *P. audax* vision using the MICA plugin. To do this, we modelled the UV and MW photoreceptors of the spider visual system using the standard D65 illuminant, and by taking into account the spectral sensitivities of the camera and the spider. The spectral sensitivity of the camera was calculated previously (sensitivities peaks were UV 369 nm, SW 477 nm, MW 556 nm, and LW 596 nm; see Robledo-Ospina et al., 2017), whereas for *P. audax* sensitivity, we used previously reported values (UV: 338 nm, MW: 544 nm) for the genus *Phidippus* (Peaslee and Wilson, 1989; de Voe, 1975). The regression model fitted well with the photoreceptor-mapping model from camera sensitivities (R^2=0.999 for both spider photoreceptors).

Spatial resolution

The spatial perception linked to the visual acuity of the observer is one of the three fundamental parameters of animal vision, together with spectral sensitivity and temporal resolution (Caves et al., 2018). We simulated the resolution (acuity) of the scene viewed by the spider at different distances from the fly (2, 4 and 8 cm; these distances were selected based on previous experiments in this system; Rao and Díaz-Fleischer, 2012). We based our analysis on the acuity correction using a Gaussian convolution from an image to simulate the spatial acuity of a given receiver through the Quantitative Colour and Pattern Analysis (QCPA) framework (van den Berg et al., 2019), which is an integrative image processing workflow in ImageJ that applies, among other parameters, spatial acuity and viewing distance correction. The minimum resolvable angle used for *P. audax* was 3.86 cycles deg^{-1} and was calculated as follows (equation modified from Reymond, 1985):

$$\mathrm{MRA} = \frac{f}{\sqrt{3} \times W_\mathrm{r} \times 57.3}, \quad (1)$$

where *f* is the focal distance and W_r is the receptor width or diameter, which for *Phidippus* are 767 and 2 µm, respectively (Land, 1969);

Journal of Experimental Biology (2022) 225, jeb244223. doi:10.1242/jeb.244223

57.3 is a conversion factor from radians to cycles deg^{-1} and assumes hexagonal packing of the photoreceptors.

We created a pseudo-colour image (for details, see Troscianko and Stevens, 2015), which is a subset of the spider vision channels without transformation, with the MW channel shown as yellow and the UV channel as blue (Fig. 5B).

Achromatic and chromatic contrasts

The details of how photoreceptors encode achromatic and colour information vary among species. However, there is evidence that in many visual systems, including arthropods such as flies and bees, the MW channel is used to provide luminance information (Cronin et al., 2014). In *Phidippus* spiders, the MW cells were the most frequently encountered type in the eye (de Voe, 1975). This high proportion may support the idea that they play an essential role in the achromatic/luminance vision (Cronin et al., 2014). The achromatic contrast (C) of the wing was estimated as the difference between the quantum catch value of the wing (q_w) and head (q_h), divided by the sum of both values, which is also known as Michelson contrast (Olsson et al., 2018):

$$C = \frac{q_w - q_h}{q_w + q_h}. \quad (2)$$

Thus, positive values indicate that the wing is perceived as brighter than the head.

We were unable to use the traditional models for signal processing in the chromatic contrast modelling (Vorobyev and Osorio, 1998) owing to a lack of information about either noise in each photoreceptor type or the subsequent neural processing of colour stimuli in *P. audax*. Hence, we estimated the perceived colour difference between head and wings independent of the achromatic mechanism for dichromatic vision, where chromatic contrast between two stimuli can be estimated in the colour space using Pythagorean distance (Renoult et al., 2015). However, for a system with only two photoreceptors, the chromaticity diagram is a segment, along such the coordinate for a stimulus (x_n) is calculated as follows:

$$\{x_n\} = \left\{ \frac{1}{\sqrt{2}} \left(s^C_{n,2} - s^C_{n,1}\right) \right\}, \quad (3)$$

where $s^C_{n,i}$ is the intensity-normalized photoreceptor signal removing the achromatic dimension:

$$s^C_{n,i} = \frac{s_{n,i}}{\sum_i s_{n,i}}, \quad (4)$$

and $s_{n,i}$ is the photoreceptor signal assuming nonlinearity regarding the photon catch value of each photoreceptor ($q_{n,i}$) applying the Weber–Fechner law:

$$s_{n,i} = \ln(q_{n,i}). \quad (5)$$

Behavioural assays

We manipulated the light environment in order to generate different wing appearances from the perspective of the spider. We used an UV-transmitting Teflon sheet as a light diffuser to enhance WICs.

Four light conditions were used for the behavioural assays, taken in a darkroom with artificial full spectrum light (Iwasaki Eye Color Arc, Venture Lighting Europe Ltd, Watford, Hertfordshire, UK). The treatments were chosen to enhance different components of the appearance of the wing and are as follows: (1) control (to enhance perception of pigmented part of the wings): white background,

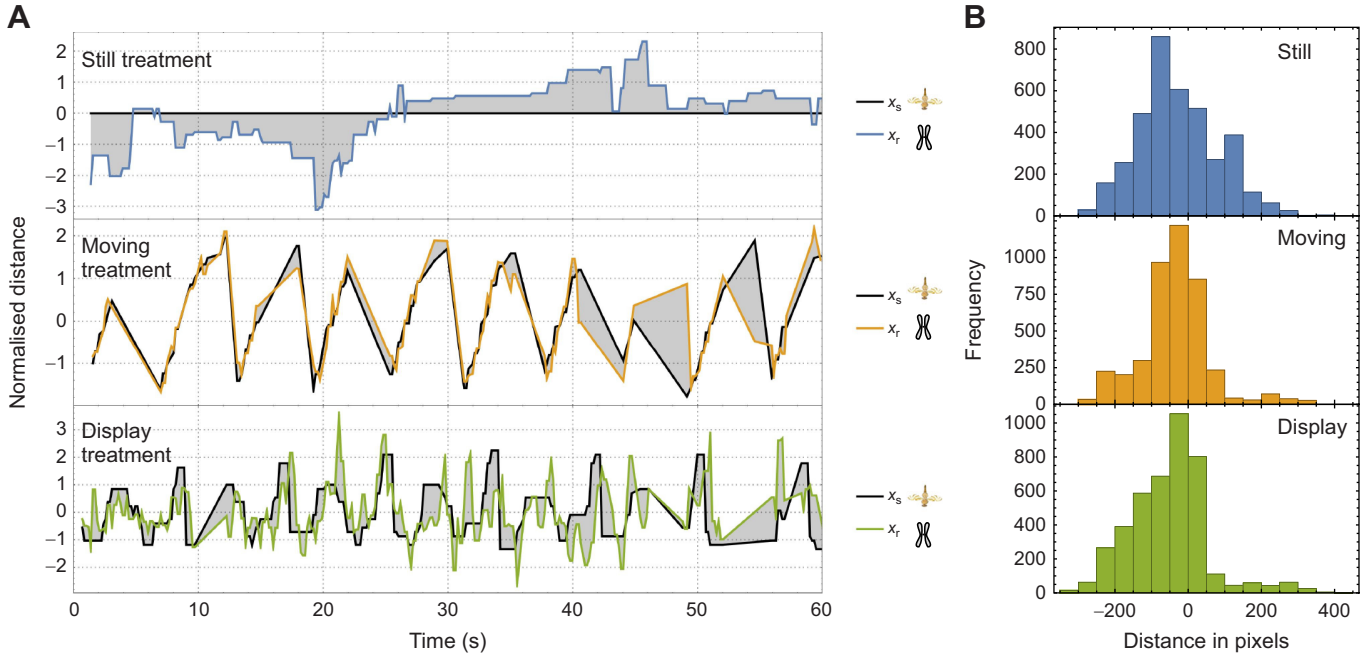

Fig. 3. Time-series analysis of the horizontal movement of stimulus and retinal response. (A) We tracked the x positions of retinae (x_r) and stimulus (x_s) in three treatments: (1) still fly (blue line), (2) moving fly (orange line) and (3) displaying fly (green line). The changes in horizontal movement over time were then normalised to have a mean of 0 and a standard deviation of 1 to facilitate comparisons between stimuli and response. The distance between the two time-series curves (shaded areas) was considered for further analysis. Perfect tracking of the stimulus would result in precisely overlapping curves. Note this is a sample figure showing responses for one spider. (B) We compared the frequency distribution of the difference in x positions (curve separation in pixels) between the curves for the three treatments for all spiders (Kolmogorov–Smirnov test). A data point at 0 on the x-axis implies that the stimulus and response curves coincided at that point. Retinae that tracked the stimulus better over the time period sampled would show a higher peak at 0. Moving flies (n=15) were better tracked; still flies (n=14) were intermediate and displaying flies (n=14) were least effectively tracked.

Journal of Experimental Biology (2022) 225, jeb244223. doi:10.1242/jeb.244223

direct light (i.e. no diffuser), light bulb without UV filter; (2) specular reflection (to enhance perception of glossy or shiny part of the wings): black background, direct light, light bulb without UV filter; (3) wing interference colours (WIC) (to enhance perception of wing interference colours): black background, diffuser between the light source and the wings, light bulb without UV filter; and (4) WIC without ultraviolet (to test whether UV plays a significant role in perception of wing interference colours): black background, diffuser, light bulb with UV filter.

With these treatments, if spiders were deterred by the presence of specular reflection or WIC, we would expect the probability of attack would be lower than in the control treatment. Furthermore, if UV played a role in deterrence, we would expect a lower attack rate for spiders encountering flies with enhanced WIC under light with a UV component in comparison to light without a UV component.

In each of these four light conditions, we recorded videos of encounters (n=15 for each treatment) between *P. audax* and *A. ludens* inside a Petri dish (15 cm diameter). Although the Petri dish transmitted UV, we have no information about other light features such as polarisation. Before the experiment began, both the spider and the fly were placed inside the Petri dish with an opaque cardboard partition (15 cm in length) in the middle for acclimatisation for 1 min. We then removed the partition and recorded the interaction for 3 min or until the spider and the fly made contact in the first interaction. We only used flies that performed the supination behaviour because previous experiments have shown that non-displaying flies are likely to be attacked at higher rates than displaying flies (Rao and Díaz-Fleischer, 2012). We quantified the number of attacks.

RESULTS

Spider orientation

In arena trials, spiders (i.e. a field of view of ±10 deg from the midpoint of the sightline) were oriented directly towards the head of both non-displaying and displaying flies. However, the distribution of the error angles between the two groups was significantly different (display group: n=342 observations, 9 spiders, mean vector μ=351.29 deg, length of mean vector r=0.898, circular s.d.=26.51 deg; non-display group: n=380 observations, 10 spiders, mean vector μ=7.2 deg, length of mean vector r=0.848, circular s.d.=32.84 deg; Watson's U^2 test, U^2=1.59, P<0.001; Fig. 1B,C).

Retinal tracking precision

In the eyetracker, the retinae of the principal eyes of the spiders were directed more closely at the heads in videos of moving flies compared with spiders that viewed videos of non-moving flies (Fig. 3A). Spiders facing displaying flies tracked the fly heads with the least precision (Fig. 3A). All distributions were significantly different from one another (Kolmogorov–Smirnov test: display versus moving, D=0.098, P<0.01; display versus still, D=0.085, P<0.05; moving versus still, D=0.072, P<0.05; Fig. 3B).

Optical flow

The different motion components (i.e. a vector flow field) of a displaying fly were substantially different from those of a moving fly (Fig. 4; Movie 3). In general, a displaying fly produced motion in different directions and magnitudes (Fig. 4A) whereas a moving fly produced motion in one direction and at lower magnitudes (Fig. 4B). With this analysis, we noted the relative stillness of the fly's head with respect to the wings and the ovipositor.

Wing interference colouration

Visual acuity and modelling

We created a composite image to show the different visual components of the fly wing (Fig. 5A). According to our simulation of the fly wing appearance (Fig. 5B), spiders were likely to detect the wing specularity and bands when at a close

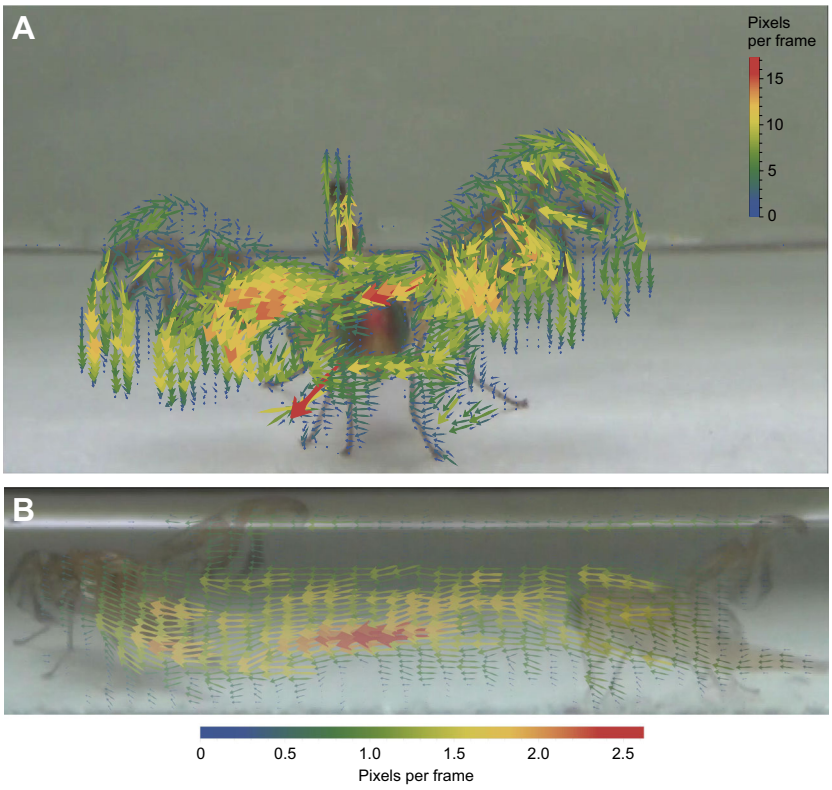

Fig. 4. Optical flow vector fields. Data are shown for (A) a displaying fly and (B) a moving fly. The arrows represent direction of the pixel displacements and colour of the arrows is coded according to the mean of the vectors (i.e. magnitude of displacement).

Journal of Experimental Biology (2022) 225, jeb244223. doi:10.1242/jeb.244223

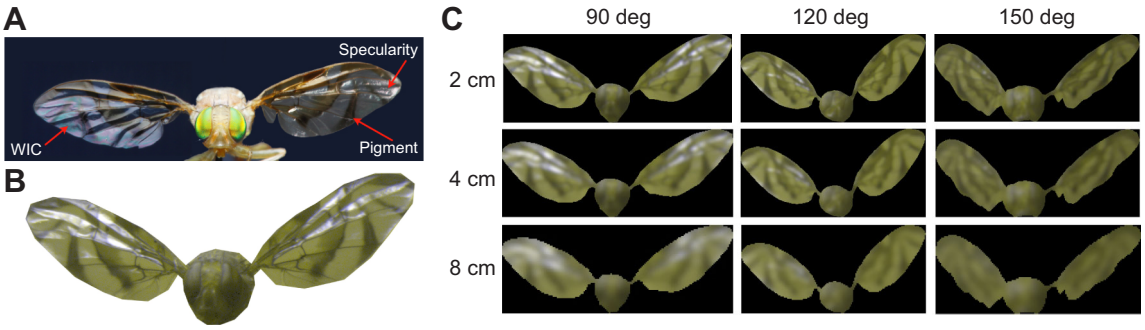

Fig. 5. Simulation of the appearance of a Mexican fruit fly (*Anastrepha ludens*) as seen from the perspective of a jumping spider. (A) Composite view of visual features showing wing specularity, wing interference colours and pigmentation. (B) Pseudo-colour image of the fly seen from the perspective of a *Phidippus audax* jumping spider's visual system at a distance of 2 cm. (C) Pseudo-colour images of different wing angles and distances.

distance and when the wing was more open (150 deg; Fig. 5C). Only the green and UV components of the total colour information produced by the transparent portion of the wing were likely to be detected by the spider, with information from the red channel unlikely to be recorded as red owing to the lack of a red receptor in this species. At greater distances (~8 cm), the overall appearance of the fly may be detected but details were not conspicuous. The percentage of wing area covered by WIC, UV and specularity in general followed a hump-shaped pattern (Fig. 6A). The data were best explained by a polynomial fit to WIC (R^2=0.82, F=9.61, P<0.05), specularity (R^2=0.71, F=5.08, P<0.05), UV (R^2=0.91, F=19.54, P<0.0001) and pigment (R^2=0.92, F=26.53, P<0.005). The significant fit suggests that information from these components is nonlinear in nature.

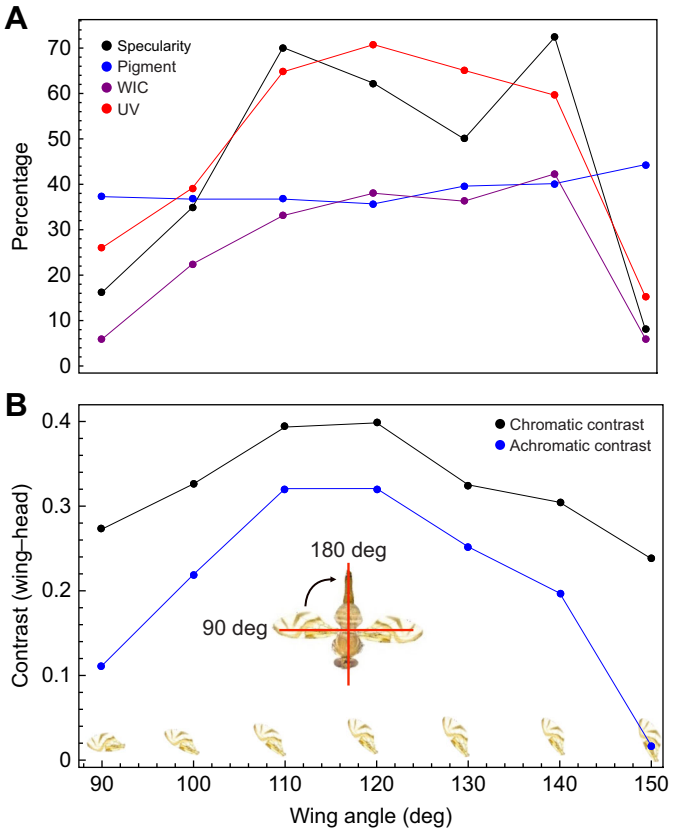

Fig. 6. Appearance of fly's wing features from a spider's perspective. (A) Apparent change in relative area of pigment, specularity, UV and wing interference colour (WIC) with opening angle of one wing. (B) Difference in achromatic and chromatic contrasts between the wing and the head with respect to opening angle of one wing. The contrast is highest when the wings are at the midpoint of display (110–120 deg). Note that the lines between the points are for visual clarity.

Achromatic and chromatic contrasts

The achromatic contrast (difference in luminance between wing and head) varied significantly according to the wing angle (polynomial fit: R^2=0.97, F=95.54, P<0.0005). The contrast followed a hump-shaped pattern, with a peak at 110–120 deg (Fig. 6B). A similar pattern was seen with the chromatic contrasts (polynomial fit: R^2=0.85, F=33.02, P<0.005; Fig. 6B). These results suggest that visual information as perceived by the spider fluctuates nonlinearly during the wing display.

Behavioural assays

There was a significant difference in the percentage of flies that were attacked in different light conditions (generalized linear regression; logit link function, binomial distribution, χ^2=8.09, d.f.=3, P<0.044). With respect to the control, flies in the WIC with UV and the WIC without UV treatments were attacked significantly less (*post hoc* contrasts; z=2.11, P<0.05 and z=2.33, P<0.05, respectively), while there was no significant difference between the specularity treatment and the control (z=−1.2, P=0.23; see Supplementary Materials and Methods for the complete model).

DISCUSSION

In this paper, we bring together three different lines of evidence that suggest that the tephritid fly's wing display generated a multitude of motion and colour cues which contributed to the hesitation by jumping spiders to attack. Using data from orientation in untethered spiders, retinal tracking in tethered spiders and visual modelling of wing appearance, we have presented a broad picture of a deterrent visual display. The deterrent effect of a tephritid fly's display against a jumping spider predator has been previously attributed to the mimetic markings on the fly's wings (Greene et al., 1987). According to this hypothesis, spiders misidentify flies as other salticid spiders. However, salticids can be deterred even when the wing markings are artificially blackened out, suggesting that the wing motion has an important deterrent effect (Rao and Díaz-Fleischer, 2012). Our results provide a mechanism that can explain this deterrence. The hesitation to attack may be attributed to the failure by the spider to accurately track the movements of the fly. In the arena experiments, there is a fluctuation in the spider's orientation when the fly is displaying, while the retina analysis showed that there was a

significant lack of precision in tracking the motion of the fly. These subtle shifts could cause the spider to slow or break off its attack, thereby allowing a displaying fly to survive an encounter with a predator (Rao and Díaz-Fleischer, 2012). In addition, the fly's head does not move as much as the ovipositor and wings when the fly is displaying, perhaps to reduce the chances of the head being detected and to attract attention to other, less vital, components. This behaviour is consistent with results from experiments on other jumping spider species that use the head component of potential prey to target attacks (Bartos and Minias, 2016). From the fly's point of view, reducing the motion of its head could allow the fly to gather more information about the nature of the threat.

To quantify the potential motion cues available from the fly movements, we calculated the optical flow of the movement from representative videos (Movie 3). The resulting vector field from the optical flow shows stark differences in magnitude and direction between a displaying fly and a moving fly. A displaying fly generates motion components in various directions and magnitudes, which may make it more difficult for the spider to quickly identify the fly as prey. A moving fly, in contrast, generates a uniform and single direction flow, which potentially makes it easier for the spider to assess the best attack angle.

The hyaline parts of wings have been recently shown to produce bright structural colouration, and it has been suggested that predators may be dissuaded from attacking insects sporting such colours (Pike, 2015). In the jumping spider–tephritid system, there are special features that we need to consider. Firstly, jumping spiders are very sensitive to movement (Drees, 1952); their principal eyes have colour vision, but their anterior lateral eyes are 'motion detection' eyes (Jakob et al., 2018). Furthermore, orientation behaviour in salticids has been shown to be mediated by the anterior lateral eyes and is influenced by the speed and size of the stimuli (Zurek et al., 2010). The supination display of the fly produces a series of motion information: the wings themselves, the changing contrasts in multiple chromatic and achromatic perspectives as the wings are extended, and the movement of the head and legs as the display is performed. Note that because we only used one wing for the visual modelling, the number of colour and movement cues produced by the fly display is likely to be doubled under natural conditions.

The behavioural assays showed that spiders are less likely to attack flies in the WIC treatment, though they are likely to use only achromatic information in targeting prey. We detected no effect of UV on the likelihood of attacks by spiders. However, we note here that a limitation of this study is that the control treatments were with a white background whereas the other treatments had a black background, which could affect the results given that there may be poorer detectability against black backgrounds. As these spiders are dichromatic, with spectral sensitivity in the UV and green wavelengths, we suggest that only achromatic contrast is being used to target prey, i.e. the spiders possibly see the colour patterns as a 'grayscale' gradient (de Voe, 1975). A similar effect may be operating in the red jumping spider *Saitis barbipes*, which does not possess a red receptor (Glenszczyk et al., 2022).

Our results may be extended to other forms of displays. Male jumping spiders use elaborate courtship displays with an abundance of motion components, and mating success is correlated with the complexity of courtship display in at least some groups (Girard et al., 2015). Given that courtship can be dangerous for males, it may be that some complex visual displays are difficult for females to quickly assess, and thus buy time for a courting male to approach. These ideas need to be tested further.

Acknowledgements
We thank Pablo Núñez Berea for help in collection of spiders in Mexico. Mary Emma Searles and Ashley Carey helped in the collection of retina data at University of Massachusetts Amherst. We thank Nathan Morehouse and David Outomuro for helpful discussions. We thank Jolyon Troscianko and two anonymous reviewers for comments that greatly improved an earlier draft of this paper. The eyetracker was designed by Cristina Canavesi and Jannick Rolland (University of Rochester) and built by Stingray Optics (Keene, North Hampshire).

Competing interests
The authors declare no competing or financial interests.

Author contributions
Conceptualization: D.R., S.M.L., E.J.; Methodology: D.R., S.M.L., L.E.R., E.J.; Formal analysis: D.R., S.M.L., H.T., A.N.; Investigation: D.R., S.M.L., K.S., S.O.A., L.E.R.; Resources: D.R., E.J.; Data curation: D.R.; Writing - original draft: D.R.; Writing - review & editing: D.R., S.M.L., A.N., E.J.; Visualization: D.R., H.T., A.N., L.E.R.; Supervision: D.R., D.R.-M., E.J.; Project administration: D.R., D.R.-M.; Funding acquisition: D.R., E.J.

Funding
This project was financed by grants from the Consejo Nacional de Ciencia y Tecnología Mexico Ciencia Básica (168746) to D.R., the National Science Foundation (IOS 0952822 and IOS 1656714) to E.J. and the Australian Research Council (FT140100221, DP150101172) to A.N.

Data availability
All relevant data can be found within the article and its supplementary information.

References
Aguilar-Argüello, S., Díaz-Fleischer, F. and Rao, D. (2015). Target-invariant aggressive display in a tephritid fly. *Behav Proc* **121**, 33-36. doi:10.1016/j.beproc.2015.10.006

Aluja, M., Piñero, J., Jácome, I., Diaz-Fleischer, F. and Sivinski, J. (2006). Behavior of flies in the genus *Anastrepha*. In *Fruit Flies (Tephritidae): Phylogeny and Evolution of Behavior* (ed. M. Aluja and A. L. Norrbom), pp. 376-401. Routledge.

Bartos, M. and Minias, P. (2016). Visual cues used in directing predatory strikes by the jumping spider *Yllenus arenarius* (Araneae, Salticidae). *Anim. Behav.* **120**, 51-59. doi:10.1016/j.anbehav.2016.07.021

Bednarski, J. V., Taylor, P. and Jakob, E. M. (2012). Optical cues used in predation by jumping spiders, *Phidippus audax* (Araneae, Salticidae). *Anim. Behav.* **84**, 1221-1227. doi:10.1016/j.anbehav.2012.08.032

Brodie, E. D. (1977). Salamander antipredator postures. *Copeia* **1977**, 523-535. doi:10.2307/1443271

Bruce, M., Daye, D., Long, S. M., Winsor, A. M., Menda, G., Hoy, R. R. and Jakob, E. M. (2021). Attention and distraction in the modular visual system of a jumping spider. *J. Exp. Biol.* **224**, jeb.231035. doi:org/10.1242/jeb.231035

Canavesi, C., Long, S., Fantone, D., Jakob, E., Jackson, R. R., Harland, D. and Rolland, J. P. (2011). Design of a retinal tracking system for jumping spiders. In *Spie Optical Engineering+Applications 2011* (ed. R. J. Koshel and G. G. Gregory), pp. 81290A–8. SPIE.

Carducci, J. and Jakob, E. (2000). Rearing environment affects behaviour of jumping spiders. *Anim. Behav.* **59**, 39-46. doi:10.1006/anbe.1999.1282

Caro, T. (1995). Pursuit-deterrence revisited. *TREE* **10**, 500-503.

Caves, E. M., Brandley, N. C. and Johnsen, S. (2018). Visual acuity and the evolution of signals. *TREE* **33**, 1-15.

Collett, T. and Land, M. (1975). Visual control of flight behaviour in the hoverfly *Syritta pipiens* L. *J. Comp. Physiol.* **99**, 1-66. doi:10.1007/BF01464710

Cronin, T. W., Johnsen, S., Marshall, N. J. and Warrant, E. J. (2014). *Visual Ecology*. Princeton University Press.

de Voe, R. D. (1975). Ultraviolet and green receptors in principal eyes of jumping spiders. *J. Gen. Physiol.* **66**, 193-207. doi:10.1085/jgp.66.2.193

Drees, O. (1952). Untersuchungen über die angeborenen Verhaltensweisen bei Springspinnen (Salticidae). *Z. Tierpsychol.* **9**, 169-207.

Eichorn, C., Hrabar, M., Ryn, E. C. V., Brodie, B. S., Blake, A. J. and Gries, G. (2017). How flies are flirting on the fly. *BMC Biol.* **15**, 1-10. doi:10.1186/s12915-016-0342-6

Girard, M. B., Elias, D. O. and Kasumovic, M. M. (2015). Female preference for multi-modal courtship: multiple signals are important for male mating success in peacock spiders. *Proc. R. Soc. B* **282**, 20152222. doi:10.1098/rspb.2015.2222

Glenszczyk, M., Outomuro, D., Gregorič, M., Kralj-Fišer, S., Schneider, J. M., Nilsson, D.-E., Morehouse, N. I. and Tedore, C. (2022). The jumping spider *Saitis barbipes* lacks a red photoreceptor to see its own sexually dimorphic red coloration. *Sci Nat* **109**, 6. doi:10.1007/s00114-021-01774-6

Gonzalez-Lopez, G. I., Rao, D., Diaz-Fleischer, F., Orozco-Dávila, D. and Perez-Staples, D. (2015). Antipredator behavior of the new mass-reared unisexual strain

of the Mexican fruit fly. *Bull. Ent. Res.* **106**, 314-321. doi:10.1017/S0007485315000966

Greene, E., Orsak, L. J. and Whitman, D. W. (1987). A tephritid fly mimics the territorial displays of its jumping spider predators. *Science* **236**, 310-312. doi:10.1126/science.236.4799.310

Harland, D. P., Li, D. and Jackson, R. R. (2012). How Jumping Spiders See the World. In *How Animals See The World: Comparative Behavior, Biology, and Evolution of Vision* (ed. O. F. Lazareva, T. Shimizu and E. A. Wasserman), pp. 133-163. Oxford University Press.

Hasson, O. (1991). Pursuit-deterrent signals: communication between prey and predator. *TREE* **6**, 325-329.

Hasson, O. (1995). A fly in spiders clothing: what size the spider? *Proc. R. Soc. B* **261**, 223-226. doi:10.1098/rspb.1995.0140

Hawkes, M. F., Duffy, E., Joag, R., Skeats, A., Radwan, J., Wedell, N., Sharma, M. D., Hosken, D. J. and Troscianko, J. (2019). Sexual selection drives the evolution of male wing interference patterns. *Proc. R. Soc. B* **286**, 20182850-8. doi:10.1098/rspb.2018.2850

Hill, D. E. (2022). Neurobiology and vision of jumping spiders (Araneae: Salticidae). *Peckhamia* **255.1**, 1-81.

Jakob, E. M., Long, S. M., Harland, D. P., Jackson, R. R., Carey, A., Searles, M. E., Porter, A. H., Canavesi, C. and Rolland, J. P. (2018). Lateral eyes direct principal eyes as jumping spiders track objects. *Curr. Biol.* **28**, R1092-R1093. doi:10.1016/j.cub.2018.07.065

Kelley, J. L., Tatarnic, N. J., Schröder-Turk, G. E., Endler, J. A. and Wilts, B. D. (2019). A dynamic optical signal in a nocturnal moth. *Curr. Biol.* **29**, 2919-2925.e2. doi:10.1016/j.cub.2019.07.005

Kjernsmo, K., Whitney, H. M., Scott-Samuel, N. E., Hall, J. R., Knowles, H., Talas, L. and Cuthill, I. C. (2020). Iridescence as camouflage. *Curr. Biol.* **30**, 551-555. doi:10.1016/j.cub.2019.12.013

Land, M. (1969). Movements of the retinae of jumping spiders (Salticidae: Dendryphantinae) in response to visual stimuli. *J. Exp. Biol.* **51**, 471-493. doi:10.1242/jeb.51.2.471

Landler, L., Ruxton, G. D. and Malkemper, E. P. (2021). Advice on comparing two independent samples of circular data in biology. *Sci. Rep.* **11**, 20337. doi:10.1038/s41598-021-99299-5

Ligon, R. A., Diaz, C. D., Morano, J. L., Troscianko, J., Stevens, M., Moskeland, A., Laman, T. G. and Scholes, E. (2018). Evolution of correlated complexity in the radically different courtship signals of birds-of-paradise. *PLoS Biol.* **16**, e24-e2006962. doi:10.1371/journal.pbio.2006962

Mather, M. H. and Roitberg, B. D. (1987). A sheep in wolf's clothing: tephritid flies mimic spider predators. *Science* **236**, 308-310. doi:10.1126/science.236.4799.308

Meijering, E., Dzyubachyk, O. and Smal, I. (2012). Methods for cell and particle tracking. *Methods Enzymol.* **504**, 183-200. doi:10.1016/B978-0-12-391857-4.00009-4

Morehouse, N. I. (2020). Spider vision. *Curr. Biol.* **30**, R975-R980. doi:10.1016/j.cub.2020.07.042

Olsson, P., Lind, O. and Kelber, A. (2018). Chromatic and achromatic vision: parameter choice and limitations for reliable model predictions. *Behav. Ecol.* **29**, 273-282. doi:10.1093/beheco/arx133

Otto, J. C. and Hill, D. E. (2017). Catalogue of the Australian peacock spiders (Araneae: Salticidae: Euophryini: Maratus, Saratus). *Peckhamia* 148, 1-21.

Parker, A. (1998). The diversity and implications of animal structural colours. *J. Exp. Biol.* **201**, 2343-2347. doi:10.1242/jeb.201.16.2343

Peaslee, A. G. and Wilson, G. (1989). Spectral sensitivity in jumping spiders (Araneae, Salticidae). *J Comp Physiol A* **164**, 359-363. doi:10.1007/BF00612995

Pike, T. W. (2015). Interference coloration as an anti-predator defence. *Biol. Lett.* **11**, 20150159. doi:10.1098/rsbl.2015.0159

Rao, D. and Díaz-Fleischer, F. (2012). Characterisation of predator-directed displays in tephritid flies. *Ethology* **118**, 1165-1172. doi:10.1111/eth.12021

Raudies, F. (2013). Optic flow. *Scholarpedia* **8**, 30724. doi:10.4249/scholarpedia.30724

Renoult, J. P., Kelber, A. and Schaefer, M. H. (2015). Colour spaces in ecology and evolutionary biology. *Biol. Rev.* **92**, 292-315. doi:10.1111/brv.12230

Reymond, L. (1985). Spatial visual acuity of the eagle Aquila audax: a behavioural, optical and anatomical investigation. *Vision Res.* **25**, 1477-1491. doi:10.1007/s10682-022-10156-x

Robledo-Ospina, L. E. and Rao, D. (2022). Dangerous visions: a review of visual antipredator strategies in spiders. *Evol. Ecol.* **36**, 163-180. doi:10.1007/s10682-022-10156-x

Robledo-Ospina, L. E., Escobar-Sarria, F., Troscianko, J. and Rao, D. (2017). Two ways to hide: predator and prey perspectives of disruptive coloration and background matching in jumping spiders. *Biol. J. Linn. Soc.* **122**, 752-764. doi:10.1093/biolinnean/blx108

Rosenthal, G. G. (2007). Spatiotemporal Dimensions of Visual Signals in Animal Communication. *Ann Rev Ecol Sys* **38**, 155-178. doi:10.1146/annurev.ecolsys.38.091206.095745

Rößler, D. C., Agrò, M. D., Kim, K. and Shamble, P. S. (2021). Static visual predator recognition in jumping spiders. *Funct. Ecol.*. **36**, 561-571. doi:10.1111/1365-2435.13953

Ruxton, G., Sherratt, T. N. and Speed, M. (2018). *Avoiding Attack: the Evolutionary Ecology of Crypsis, Warning Signals and Mimicry*, 2nd edn. Oxford University Press.

Schultz, T. D. and Fincke, O. M. (2009). Structural colours create a flashing cue for sexual recognition and male quality in a neotropical giant damselfly. *Funct. Ecol.* **23**, 724-732. doi:10.1111/j.1365-2435.2009.01584.x

Shevtsova, E., Hansson, C., Janzen, D. H. and Kjaerandsen, J. (2011). Stable structural color patterns displayed on transparent insect wings. *Proc. Natl. Acad. Sci. USA* **108**, 668-673. doi:10.1073/pnas.1017393108

Stuart-Fox, D., Ospina-Rozo, L., Ng, L. and Franklin, A. M. (2020). The paradox of iridescent signals. *TREE* **6**, 1-9.

Troscianko, J. and Stevens, M. (2015). Image calibration and analysis toolbox – a free software suite for objectively measuring reflectance, colour and pattern. *Methods Ecol. Evol.* **6**, 1320-1331. doi:10.1111/2041-210X.12439

van den Berg, C. P., Troscianko, J., Endler, J. A., Marshall, N. J. and Cheney, K. L. (2019). Quantitative colour pattern analysis (QCPA): a comprehensive framework for the analysis of colour patterns in nature. *Methods Ecol. Evol.* **11**, 316-332. doi:10.1111/2041-210X.13328

Vorobyev, M. and Osorio, D. (1998). Receptor noise as a determinant of colour thresholds. *Proc. R. Soc. B* **265**, 351-358. doi:10.1098/rspb.1998.0302

Winsor, A. M., Pagoti, G. F., Daye, D. J., Cheries, E. W., Cave, K. R. and Jakob, E. M. (2021). What gaze direction can tell us about cognitive processes in invertebrates. *Biochem. Biophys. Res. Commun.* **87**, 12-39. doi:10.1016/j.bbrc.2020.12.001

Zurek, D. B., Taylor, A. J., Evans, C. S. and Nelson, X. J. (2010). The role of the anterior lateral eyes in the vision-based behaviour of jumping spiders. *J. Exp. Zool. A* **213**, 2372-2378. doi:10.1242/jeb.042382

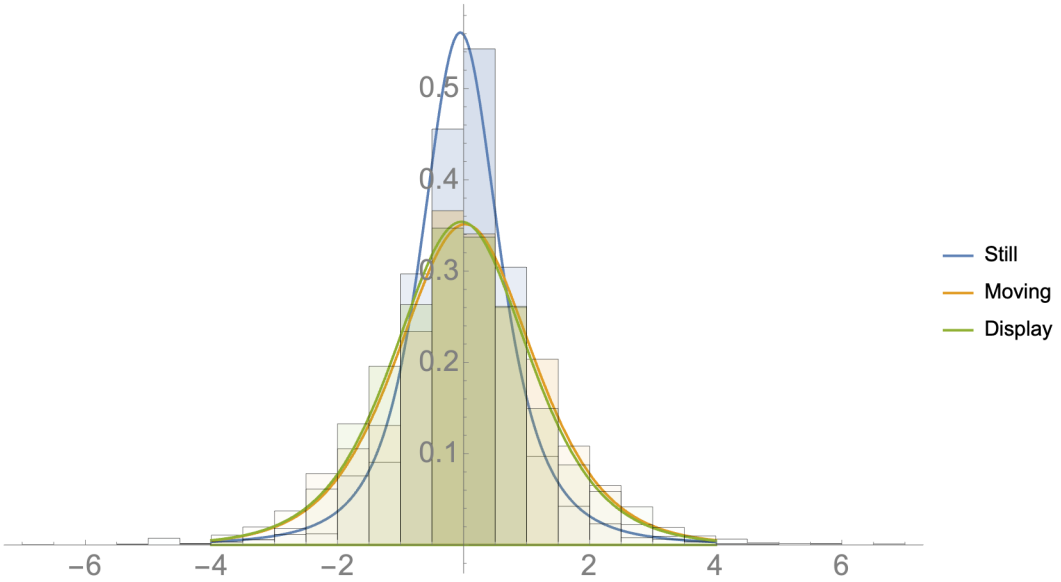

Fig. S1. Results of a Kolomogorov Smirnov test looking at the distribution of the distance between the spider retinal midpoint and the stimulus (head of the fly) in the y axis (vertical displacement). All distributions were significantly different from one another (Kolmogorov Smirnov test: Display vs Moving, $D = 0.037$, $p < 0.006$; Display vs Still, $D = 0.11$, $p < 0.0001$; Moving vs Still, $D = 0.123$, $p < 0.0001$). In comparison with the horizontal axis, there was very little vertical displacement. These results suggest that in the vertical axis, spiders were more likely to coincide with the position of the fly in the still treatment, whereas there were similar levels of frequency in the displaying and the moving treatments.

Supplementary Materials and Methods

Generalized Linear Models

ModelInfo

Info	Value	Comment
Model Type	Logistic	Model for binary y
Link function	logit	log odd of attack=1
Distribution	Binomial	Dichotomous event distribution of y
R-squared	0.120	Proportion of reduction of error
AIC	67.257	Less is better
Deviance	59.257	Less is better
Residual DF	47	
Converged	yes	A solution was found

Analysis of Deviance: Omnibus Tests

	X^2	df	p
treatment	8.09	3	0.044

Model Coefficients (Parameter Estimates)

				95% Confidence Interval				
	Contrast	Estimate	SE	Lower	Upper	exp(B)	z	p
(Intercept)	Intercept	-0.602	0.326	-1.282	0.0177	0.548	-1.847	0.065
treatment1	Shine - (Control, Shine, WIC, WICnoUV)	0.314	0.502	-0.686	1.3106	1.369	0.626	0.531
treatment2	WIC - (Control, Shine, WIC, WICnoUV)	-0.602	0.568	-1.832	0.4617	0.548	-1.059	0.289
treatment3	WICnoUV - (Control, Shine, WIC, WICnoUV)	-1.007	0.637	-2.486	0.1303	0.365	-1.581	0.114

PostHocTests

Post Hoc Comparisons-treatment

Comparison						
treatment		treatment	Difference	SE	z	p
Control	-	Shine	2.67	2.18	1.201	0.230
	-	WIC	6.67	5.99	2.110	0.035
	-	WICnoUV	10.00	9.87	2.332	0.020
Shine	-	WIC	2.50	2.13	1.076	0.282
	-	WICnoUV	3.75	3.54	1.400	0.162
WIC	-	WICnoUV	1.50	1.52	0.399	0.690

Estimated Marginal Means

treatment

			95% Confidence Interval	
treatment	**Prob**	**SE**	**Lower**	**Upper**
Control	0.667	0.136	0.3759	0.869
Shine	0.429	0.132	0.2065	0.684
WIC	0.231	0.117	0.0763	0.522
WICnoUV	0.167	0.108	0.0420	0.477

Effects Plots

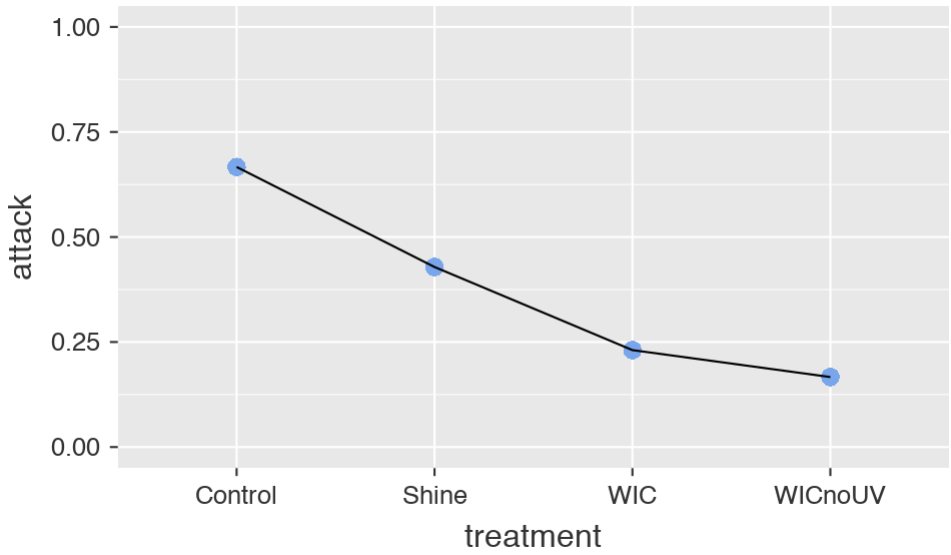

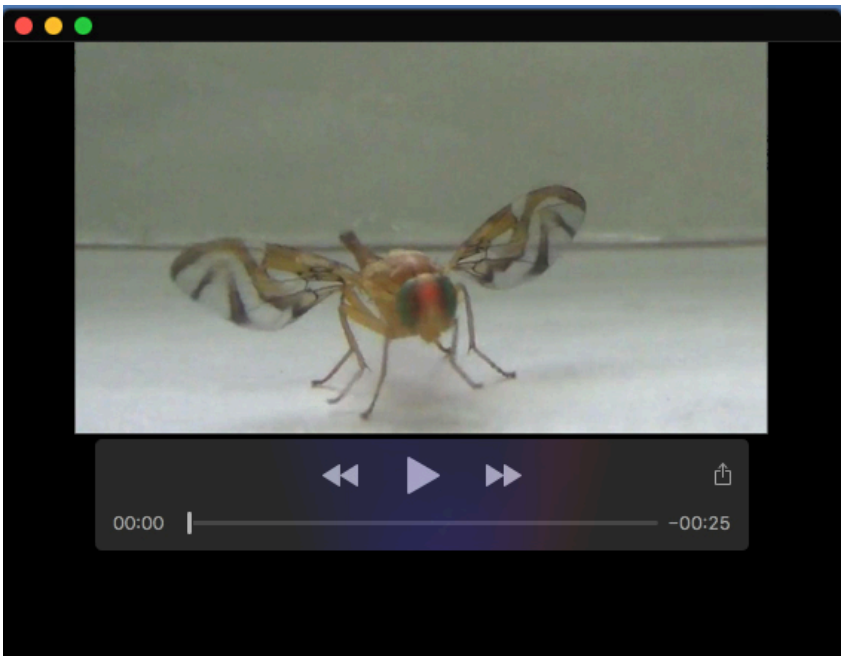

Movie 1. Video showing supination display of the Mexican fruit fly (*Anastrepha ludens*) against a jumping spider predator (*Phidippus audax*).

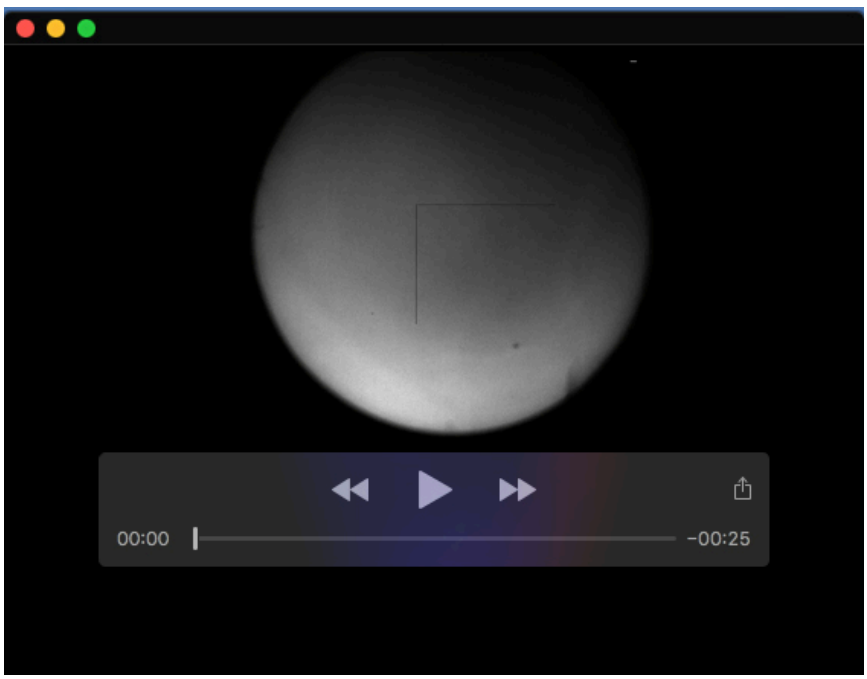

Movie 2. Sample video showing the response of the spider retinae overlaid with that of a displaying fly.

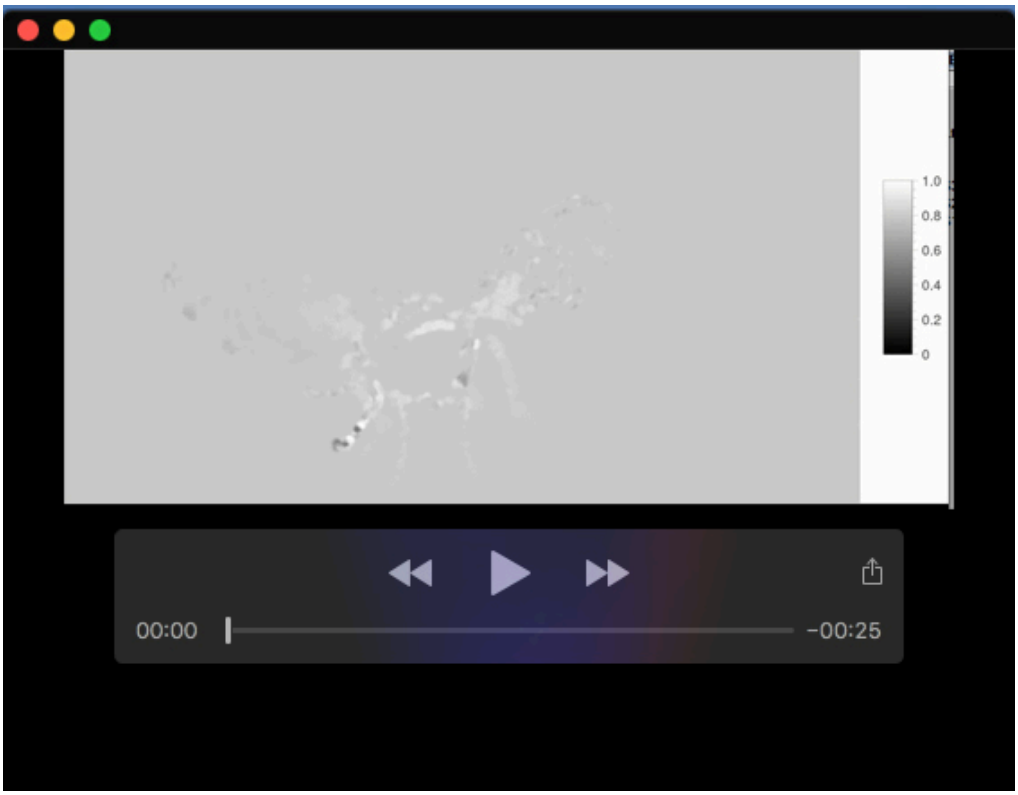

Movie 3. Video showing pixel displacement of a displaying fly and a moving fly. The videos are colour coded according to magnitude of displacement, with lighter pixels showing higher displacement and darker pixels showing lower displacement. See Fig. 4 for a vector field representation of these videos.